

Accepted Manuscript

Mathematical modelling of a tidal power station with diesel and wind units

Alexander Baykov, Andrey Dar'enkov, Andrey Kurkin, Elena Sosnina

PII: S1018-3647(18)31876-7

DOI: <https://doi.org/10.1016/j.jksus.2019.01.009>

Reference: JKUS 786

To appear in: *Journal of King Saud University - Science*

Received Date: 23 October 2018

Accepted Date: 17 January 2019



Please cite this article as: A. Baykov, A. Dar'enkov, A. Kurkin, E. Sosnina, Mathematical modelling of a tidal power station with diesel and wind units, *Journal of King Saud University - Science* (2019), doi: <https://doi.org/10.1016/j.jksus.2019.01.009>

This is a PDF file of an unedited manuscript that has been accepted for publication. As a service to our customers we are providing this early version of the manuscript. The manuscript will undergo copyediting, typesetting, and review of the resulting proof before it is published in its final form. Please note that during the production process errors may be discovered which could affect the content, and all legal disclaimers that apply to the journal pertain.

Mathematical modelling of a tidal power station with diesel and wind units

Alexander Baykov¹, Andrey Dar'enkov¹, Andrey Kurkin^{1,*} and Elena Sosnina¹

¹ Nizhny Novgorod State Technical University n.a. R.E. Alekseev; fae@nntu.ru

* Correspondence: aakurkin@gmail.com

Abstract: Hybrid power plants with renewable sources, having different frequencies and voltages of generated electricity, require coordination of its parameters on the basis of semiconductor converters. This causes the appearance of current and voltage harmonics in the electrical network. Analysis of the power characteristics of a hybrid power plant based on mathematical modeling will allow one to properly develop the power plant structure and select the parameters of the individual elements of its power part and control system. The article is devoted to the application of mathematical modeling for the analysis of the generated energy quality of a tidal power station with auxiliary diesel and wind units. The mathematical models for the analysis of the power indices of a tidal power station with diesel- wind aggregates are presented. Various designs of a power electrical part based on power electronic converters of electric power parameters having a microprocessor control system are considered. A detailed possibility analysis of the tidal aggregates operating modes is illustrated.

Keywords: mathematical model; tidal power station; diesel generator; wind power unit; synchronous machine; power indices

1. Introduction

The development of world energy in the XXI century involves an active use of renewable energy: mechanical wind energy and water flows, thermal and radiant energy of solar radiation and heat of the Earth, chemical energy contained in biomass [1, 2]. Renewable energy sources are still inferior to traditional sources in terms of cost and scale of production, but this difference is steadily decreasing with its development [3, 4].

Marine energy resources [5] have huge reserves of energy – solar radiation absorbed by water, kinetic energy of sea waves [6, 7], currents, tides [8] and surf. At present there are spheres of their economically profitable use – when replacing diesel generators that supply electric power to autonomous consumers on islands, along a remote coastal zone, etc. Despite the lack of potential energy resources of the seas and oceans, these technologies have not yet received its wide use. Their intensive application is hampered by natural shortcomings: large capital costs, intermittent and random nature of energy generation [9–11]. Therefore, wave, tidal and other marine power plants are connected to centralized electrical networks [12]. In case of an autonomous operation, just in parallel with them, batteries [13] or aggregates based on other sources of renewable energy, (usually wind and solar) are functioning [14, 15].

Mathematical and computer modeling is widely used for the study of such complexes.

Many scientific papers are devoted to the modeling of tidal power plant components. The task of improving energy conversion aggregates is solved in [16-18]. The tidal turbine modeling and fault diagnosis is carried out in MATLAB/Simulink in [19]. The paper [20] deals with the modeling and control of a tidal stream generator for marine renewable energy. The paper [21] focuses on the hydrodynamic performance of different forms of the duct which could accelerate the velocity of tidal flow.

The scientific papers devoted to modeling the entire system of a tidal power plant contribute to the solution of the problem. Mathematical modeling provides an opportunity to analyze energy and other technical and economic indicators. In particular, a variable nature of the frequencies and voltage levels of the generated electric power necessitates the coordination of its parameters with the use of power electronic converters. But they, in their turn, can worsen the harmonic composition of currents and

voltages [22, 23]. The effect of the variation in tides on the power quality in stand-alone network is illustrated via simulation in [24].

Papers on the modeling of hybrid generation systems can be referred to a separate group. The paper [25] studies a network presenting a rural load, such as a small village, fed from a hybrid wind/tidal turbines that are connected to a weak grid. The paper [26] deals with the development of real time simulation for a hybrid wind - tidal power system.

It is necessary to work out technical solutions, both in the structure of power plants, and in the choice of the parameters of individual units and elements of the power part and control. Thus the authors have presented the results of the development of a mathematical modeling environment for a wind-diesel power station [27], which are supplemented by a tidal aggregate with the operating modes and efficient analysis methods.

2. Methods

To analyze various electromechanical and electromagnetic processes in autonomous power plants a structural scheme (Fig. 1) is adopted, including three energy generation channels – diesel (d), wind (w) and tidal (t) equivalent to an active-inductive three-phase load (l), a backup source on the battery (Ac) and the common dc bus (dc). Energy sources—a diesel D , a wind wheel W and a tidal aggregate T rotate the shafts of the generators with frequencies $\omega_d, \omega_w, \omega_t$, developing the moments h_d, h_w, h_t . Instead of electromechanical energy converters, synchronous generators with permanent magnets (M_d, M_w) and M_t – with a controlled exciter (V_T) are used as an option.

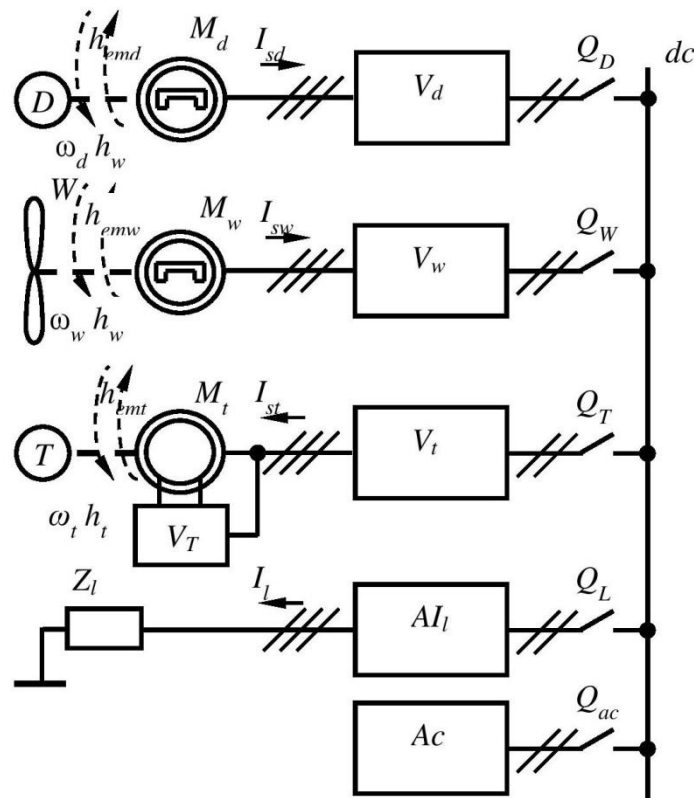


Figure 1. Structural diagram of an autonomous power plant: D, W, T – diesel, wind wheel, turbine, M_d, M_w, M_t – generators and V_d, V_w, V_t – rectifiers of diesel generator, wind and tidal channels; V_T – controlled rectifier excitation of the synchronous generator M_t ; Ai_l, Z_l – autonomous voltage inverter and equivalent load impedance; Ac – rechargeable battery; Q – switches; dc – bus direct current.

Three-phase currents of stator generators (I_{sd}, I_{sw}, I_{st}) are converted into constants by controlled and uncontrolled rectifiers (V_d, V_w, V_t). The use of the uncontrolled rectifiers is explained by connecting

an autonomous inverter to the output. Depending on the situation with the load demand, wind speed and the parameters of the tidal channel, the operator switches ($Q_d, Q_w, Q_t, Q_l, Q_{ac}$) to make the various schemes of the power plant operation work.

The tidal channel, which is the main and the most powerful, for example 400 kW, like the Vislogub tidal power station [5], provides the operation in various turbine and pumping modes. To generalize, a direct pumping mode of the tidal aggregate is of interest. It works as an asynchronous motor and operates the pump to take water from the sea into the basin which stores energy. If we assume that at this time the consumption is 100 kW, and the capacity of the wind channel is 200 kW, then the power consumption of the tidal channel will be 100 kW. The tidal channel converter operates in the autonomous voltage inverter mode. Thus, the calculation scheme for reproducing processes in the power circuit (Fig. 2) is supposed to use mathematical models of the synchronous generator, the asynchronous motor, the rectifier and the autonomous voltage inverter, i.e. a fairly wide range of models of objects.

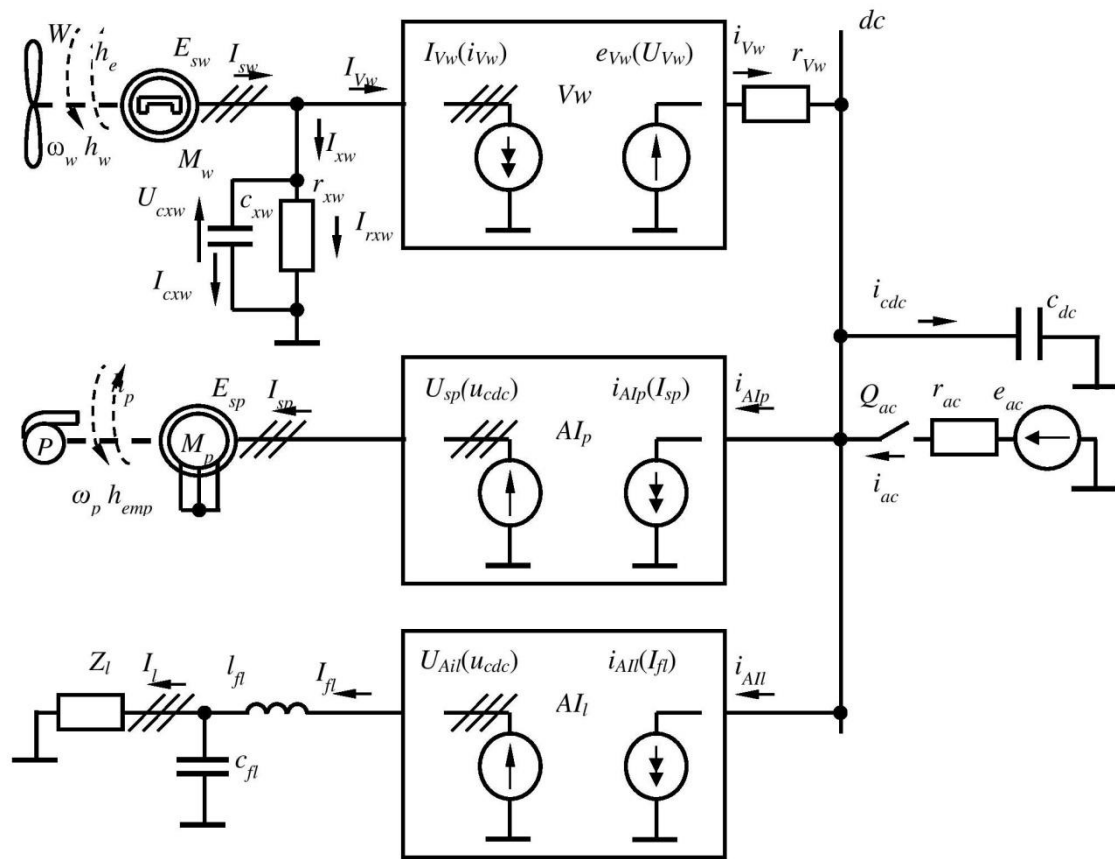


Figure 2. The design scheme of an autonomous power plant with power from the wind channel of a load and a tidal unit operating in the mode of a direct pump: W, P is a wind and a pump, M_w, V_w is a synchronous generator with permanent magnets and a wind channel rectifier, M_p – is a tidal channel machine operating in an asynchronous motor mode; AI_p, AI_l – autonomous voltage inverters of the tidal channel and load circuit; Z_l is the equivalent impedance of the load circuit r_{xw}, r_{Vw}, c_{xw} – active resistances and capacities of communication circuits; l_{fl}, c_{fl} – inductance and capacity of the load filter; Q_{ac}, r_{ac}, e_{ac} – switch, resistance and EMF (Electromagnetic field) of the battery; dc - dc bus with c_{dc} capacity.

The mathematical model of the wind turbine is described in [27].

To analyze the energy parameters of the circuit, it is possible to simplify the representation of the power electronic circuits, as ideal voltage converters of a three-phase alternating current to a constant

one and back [29]. It is advisable to single out the influence of the processes of gates commutation on the shapes of currents and voltages in a separate problem and to carry out in private design schemes of a smaller size. Therefore, it is possible to describe the functioning of complex multi-circuit circuits with key elements by simple nodes based on the dependent current and voltage sources (V_w, AI_p, AI_l).

3. Results

In the wind channel circuit, the uncontrolled rectifier V_w switches valves in six sections on the EMF period of the generator M_w in accordance with the values of the line voltages, thereby performing a functional conversion of the voltages U_{cxw} at the rectifier input to the pulsating DC power supply

$$e_{V_w} = [X_V U_{cxw}]_{j_{\max}}, \quad X_V = \begin{bmatrix} 1 & -1 & 0 \\ 1 & 0 & -1 \\ 0 & 1 & -1 \\ -1 & 1 & 0 \\ -1 & 0 & 1 \\ 0 & -1 & 1 \end{bmatrix}, \quad (1)$$

where X_V is a topological matrix providing calculation of linear voltages at the output of the three-phase bridge rectifier; j_{\max} is the number of the line corresponding to the maximum value of the vector $X_V U_{cxw}$. The capacitances C_{xw} correspond to either the filter capacitors, if present in the actual circuit, or to the specially introduced capacitances of the stator coupling circuit of the machine and the connected external circuit. In both cases, it connects in parallel the coupling resistance r_{xw} of a large value, which matches the stator circuit of the machine and the rectifier input circuit by determining the ratio between the currents

$$I_{cxw} = I_{sw} - I_{V_w} - r_{xw}^{-1} U_{cxw}. \quad (2)$$

The vector of the stator currents of the generator I_{V_w} , is assumed to be dependent on the output current of the rectifier and is determined by a similar functional transformation

$$I_{V_w} = [X_V i_{V_w}]_{j_{\max}} \quad (3)$$

based on the choice of the string j_{\max} from the vector $X_V i_{V_w}$. In its turn, the output of the rectifier is switched on by a small resistance r_{V_w} , so that the rectifier circuits V_w and DC cdc are matched:

$$i_{V_w} = r_{V_w}^{-1} (e_{V_w} - u_{cdc}). \quad (4)$$

The capacity of cdc can be present in the circuit as a filter element, or it should be included artificially with a small parameter value.

The consumed input currents (i_{AIp} , i_{AIl}) of the units of the autonomous pump inverters of the tidal aggregate and the equivalent load are determined by the stator M_p currents I_{sp} and I_{fl} and the load circuit filter inductances

$$\begin{aligned} i_{AIp} &= \text{diag}[x_{p1} \quad x_{p3} \quad x_{p5}] I_{sp}, \\ i_{AIl} &= \text{diag}[x_{l1} \quad x_{l3} \quad x_{l5}] I_{fl}, \end{aligned} \quad (5)$$

where the diagonal matrix is composed of the values of the control functions of the transistors of the odd or even group of the three-phase bridge circuit. It is assumed that if a control pulse is available, the value of the corresponding function is equal to one, otherwise it is zero. The definition of these functions is determined on the well-known vector control algorithm based on the principle of pulse width modulation.

According to the law of frequency control, the amplitudes of the voltage vector components U_{Aip} on the stator of the Mp machine operating in the asynchronous motor mode, depend on the frequency f_{sp} of the generated voltage

$$u_{Aip} = \sqrt{2} \frac{u_{snomp} f_{sp}}{f_{snom}} = \frac{u_{s \max p} f_{sp}}{f_{snom}}, \quad (6)$$

where u_{snom} , f_{snom} is the nominal effective value and frequency of the phase voltage of the machine. Similarly, the frequency of the load voltage f_l is the amplitude of the voltage vector U_{Ail}

$$u_{Ail} = \sqrt{2} \frac{u_{noml} f_l}{f_{lnom}} = \frac{u_{\max l} f_l}{f_{lnom}}. \quad (7)$$

The rotation of the vectors U_{Aip} and U_{Ail} with the corresponding angular frequencies ω_p and ω_l occurs in six sectors. The position of the formed vector of length u_{Aij} ($j = p, l$) is determined within the current sector by the k_{sect} angle φ_j (Fig. 3). This angle is calculated at discrete instants of time t_n , counted in units of measurement of simulation time and coinciding with the modulation cycles,

$$\varphi_j = \frac{2\pi\omega_j(t_n - t_{nTj})}{T_j} - (k_{sect} - 1)\frac{\pi}{3}, \quad (8)$$

where t_{nTj} is the time instant corresponding to the beginning of the reproduced period T_j of the frequency voltage f_j .

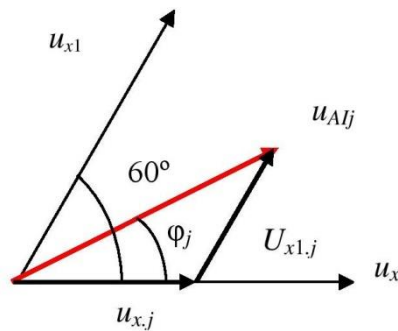


Figure 3. Formation of the current position of the voltage vector.

The ratio of the generating vector lengths $u_{x,j}$ and $u_{x1,j}$ to the base vector lengths

$$u_{Bj} = \frac{2}{3} u_{\max j} = \frac{2}{3} u_{x,j} = \frac{2}{3} u_{x1,j} \quad (9)$$

determines the duty cycle

$$\gamma_{x,j} = \frac{u_j}{u_{Bj}} \frac{(\cos \varphi_j - \sin \varphi_j)}{\sqrt{3}}, \gamma_{x+1,j} = \frac{u_j}{u_{Bj}} \frac{2 \sin \varphi_j}{\sqrt{3}}. \quad (10)$$

Using the rounding operation, we calculate the numbers of cycles $k_{x,j}$, $k_{x+1,j}$ and $k_{0,j}$ for these vectors and for the zero interval within the T_{shim} PWM (Pulse width modulation) modulation period which consists of a number of cycles

$$k_{x,j} = \text{round} \left(\frac{\gamma_{x,j} T_{shim}}{dt_{tact}} \right), k_{x+1,j} = \text{round} \left(\frac{\gamma_{x+1,j} T_{shim}}{dt_{tact}} \right), k_{0,j} = \frac{T_{shim}}{dt_{tact}} - k_{x,j} - k_{x+1,j}. \quad (11)$$

The generating vectors are formed by combinations of open and closed transistors that coincide with the combinations of control pulses X_j according to Table 1.

Table 1. Formation of control pulses by sector intervals

k_{sect}	Pulses						
	Vectors	x_1	x_2	x_3	x_4	x_5	x_6
1	X	1	0	0	1	0	1
	X_1	1	0	1	0	0	1
	X_0	1	0	1	0	1	0
2	X	1	0	1	0	0	1
	X_1	0	1	1	0	0	1
	X_0	0	1	0	1	0	1
3	X	0	1	1	0	0	1
	X_1	0	1	1	0	1	0
	X_0	1	0	1	0	1	0
4	X	0	1	1	0	1	0
	X_1	0	1	0	1	1	0
	X_0	0	1	0	1	0	1
5	X	0	1	0	1	1	0
	X_1	1	0	0	1	1	0
	X_0	1	0	1	0	1	0
6	X	1	0	0	1	1	0
	X_1	1	0	0	1	0	1
	X_0	0	1	0	1	0	1

In the next calculation step, after determining the sector, the PWM period and the interval inside it, control pulse vectors X_j are set, which have already been used in (5) to calculate the input currents of the inverters. They are also used to calculate three-phase voltages at the output of the inverter of a tidal aggregate

$$\begin{aligned} U_{sp} &= 0, \text{ if } x_2 + x_4 + x_6 = 0, \\ U_{sp} &= 0, \text{ if } x_2 + x_4 + x_6 = 3, \\ U_{sp} &= \left(-\text{diag}(x_1 \ x_3 \ x_5) + \frac{2}{3} \right) u_{cdc}, \text{ if } x_2 + x_4 + x_6 = 1, \\ U_{sp} &= \left(\text{diag}(x_2 \ x_4 \ x_6) - \frac{2}{3} \right) u_{cdc}, \text{ if } x_2 + x_4 + x_6 = 2, \end{aligned} \quad (12)$$

where the values of the key management functions of the analyzed inverter are used, and in the case of the load channel, the stress vector indices the change from "sp" to "All".

An important advantage of the described algorithm for modeling vector control of autonomous voltage inverters is the speed that does not exclude accounting for discreteness not only in the modulation frequency of PWM (20 kHz), but also in clock frequency.

4. Discussion

The functioning of electromechanical processes in the circuit (Fig. 2) is described on the basis of the application of the Park-Gorev coordinate transformations [29]. Equations of the state of a wind channel with neglect of the effect of compensating circuits in static modes

$$\begin{aligned}
 \frac{d}{dt} \psi_{dw} &= -\omega_{rw} \psi_{qw} - r_{sw} i_{dw} - u_{dcxw}, \\
 \frac{d}{dt} \psi_{qw} &= \omega_{rw} (\psi_{dw} + \psi_{fw}) - r_{sw} i_{qw} - u_{qcxw}, \\
 \frac{d}{dt} \omega_{rw} &= j_w^{-1} (h_w - h_{emw}), \\
 \frac{d}{dt} \theta_{rw} &= \omega_w, \\
 \frac{d}{dt} U_{cxw} &= c_{xw}^{-1} I_{cxw}
 \end{aligned} \tag{13}$$

have as independent variables: ψ_{dw} , and ψ_{qw} are flux linkages of a two-phase equivalent machine along the longitudinal transverse axis; ω_w and θ_w - are the rotational speed and rotational angle of the rotor, U_{cxw} - is the voltage vector of the capacitances of the communication circuit. The linkage of the permanent magnet of the rotor ψ_{fp} is a parameter. The right-hand sides of equation (13) are calculated using relations

$$\begin{aligned}
 I_{dqw} &= \begin{bmatrix} l_{dw}^{-1} & 0 \\ 0 & l_{qw}^{-1} \end{bmatrix} \begin{bmatrix} \psi_{dw} \\ \psi_{qw} \end{bmatrix}, U_{dqxw} = \begin{bmatrix} u_{dxw} \\ u_{qxw} \end{bmatrix} = A_{dqw} \begin{bmatrix} U_{cxw.1} \\ U_{cxw.2} \end{bmatrix}, \\
 h_{emw} &= 1,5 i_{qw} \psi_{fw} \\
 I_{sw} &= A_{dqw}^{-1} I_{dqw}, I_{xw} = I_{sw} - I_{vw}, I_{rxw} = r_{xw}^{-1} U_{cxw}, I_{cxw} = I_{xw} - I_{rxw}, \\
 A_{dqw} &= 2/\sqrt{3} \begin{bmatrix} \sin(\theta_{rw} + \pi/3) & \sin(\theta_{rw}) \\ \cos(\theta_{rw} + \pi/3) & \cos(\theta_{rw}) \end{bmatrix},
 \end{aligned} \tag{14}$$

where l_{dw} , l_{qw} , r_{sw} - is the stator inductance of the M_w machine along the longitudinal and transverse axes and the active resistance of the stator winding; j_w - is the moment of inertia of the wind power unit.

A similar equation would be for the generator M_p of the channel of the tidal aggregate in the turbine mode. In the same mode of the induction motor driving the pump, its equation of state has the form

$$\begin{aligned}
 \frac{d}{dt} \Psi_{dqsp} &= U_{dqsp} + \omega_{sp} B \Psi_{dqsp} - r_{sp} I_{dqsp}, \\
 \frac{d}{dt} \Psi_{dqrp} &= (\omega_{sp} - \omega_{rp}) B \Psi_{dqrp} - r_{rp} I_{dqrp}, \\
 \frac{d\omega_{rp}}{dt} &= j_{rp}^{-1} (h_{emp} - h_p), \\
 \frac{d\theta_{rp}}{dt} &= \omega_{rp},
 \end{aligned} \tag{15}$$

where Ψ_{dqsp} , and Ψ_{dqrp} are the stator and rotor flux linkages of the two-phase equivalent machine M_p along the longitudinal transverse axis; ω_p and θ_p – rotational speed and rotor angle. The right-hand sides of equation (15) are calculated using (12) and relations:

$$\begin{aligned}
 A_{dqsp} &= 2/\sqrt{3} \begin{bmatrix} \sin(\theta_{sp} + \pi/3) & \sin(\theta_{sp}) \\ \cos(\theta_{sp} + \pi/3) & \cos(\theta_{sp}) \end{bmatrix}, \theta_{sp} = \omega_{sp} t, B = \begin{bmatrix} 0 & -1 \\ 1 & 0 \end{bmatrix}, \\
 U_{dqsp} &= A_{dqsp} \begin{bmatrix} u_{sp,1} \\ u_{sp,2} \end{bmatrix}, I_{dqsrp} = L_{srp}^{-1} \begin{bmatrix} \Psi_{dqsp} \\ \Psi_{dqrp} \end{bmatrix} = \begin{bmatrix} I_{dqsp} \\ I_{dqrp} \end{bmatrix} = \begin{bmatrix} i_{dsp} \\ i_{qsp} \\ i_{drp} \\ i_{qrp} \end{bmatrix}, L_{srp} = \begin{bmatrix} l_{sp} & 0 & l_m & 0 \\ 0 & l_{sp} & 0 & l_m \\ l_m & 0 & l_{rp} & 0 \\ 0 & l_m & 0 & l_{rp} \end{bmatrix}, \\
 h_{emp} &= l_m (i_{qsp} i_{drp} - i_{dsp} i_{qrp}), I_{sp} = H_1^{-1} A_{dqsp}^{-1} I_{dqsp},
 \end{aligned} \tag{16}$$

where l_{sp} , l_{rp} , r_{sp} , r_{rp} – are the inductances and the active resistances of the stator and rotor windings of the M_p machine in the operating mode of the induction motor; j_p – is the moment of inertia of the tidal aggregate.

Equation of state of three-phase equivalent active-inductive load r_l - l_l :

$$\begin{aligned}
 \frac{d}{dt} I_{hl} &= L_{hl}^{-1} (U_{hcfl} - R_{hl} I_{hl}), \\
 \frac{d}{dt} I_{All} &= l_{fl}^{-1} (U_{All} - U_{hcfl} - r_{fl} I_{All}), \\
 \frac{d}{dt} U_{cfl} &= c_{fl}^{-1} (I_l - I_{All})
 \end{aligned} \tag{17}$$

has as independent variables the loop currents I_{hl} of the load circuit, the currents I_{fl} of inductances and the voltage of the capacitances U_{cfl} of the filter having the parameters l_{fl} , r_{fl} , c_{fl} . The right-hand sides of (17) are calculated taking into account (12) and relations

$$\begin{aligned}
 U_{chl} &= H_1 U_{cfl}, I_l = H_1^{-1} I_{hl}, H_1 = \begin{bmatrix} 1 & 0 & -1 \\ 0 & 1 & -1 \end{bmatrix}, \\
 L_{hl} &= H_1 \begin{bmatrix} l_l & 0 & 0 \\ 0 & l_l & 0 \\ 0 & 0 & l_l \end{bmatrix} H_1^{-1}, R_{hl} = H_1 \begin{bmatrix} r_l & 0 & 0 \\ 0 & r_l & 0 \\ 0 & 0 & r_l \end{bmatrix} H_1^{-1}.
 \end{aligned} \tag{18}$$

The DC bus connecting the circuit channels has at least one inertial parameter- the capacitance C_{dc} , which can be a real capacitor filter battery, or an artificially introduced small communication capacitance. The equation of state of the voltage of this capacitance is expressed using the results of the calculation of the power supply EMF at the outlet of the wind channel (1) and the currents consumed by the pump channel of the tidal unit and the equivalent load (5):

$$\frac{du_{cdc}}{dt} = C_{dc}^{-1} \left(r_{Vw}^{-1} (e_{Vw} - u_{cdc}) - i_{AIp} - i_{All} \right). \quad (19)$$

An important stage in the analysis of the effectiveness of the technical solutions being adopted is the determination of integral indicators of the quality of the functioning of devices. For the analysis of the most important of them – energy indices a harmonic analysis of the curves of the functions F of the phase currents I_j and the voltage U_j is provided. When reproducing the corresponding processes, these curves are obtained as arrays from the values $F_{j(n)}$ ($n = 1, 2, \dots, N_{dt}$) on the period T with the same step dt . The harmonic components of the phase currents and voltages are found from the formulae:

$$F_{A.j(k)} = \sum_{n=1}^{N_{dt}} F_{j(n)} \cos \left(k 2\pi \frac{1}{T} n \cdot dt \right), \quad (20)$$

$$F_{B.j(k)} = \sum_{n=1}^{N_{dt}} F_{j(n)} \sin \left(k 2\pi \frac{1}{T} n \cdot dt \right).$$

In the case of symmetry of the phase parameters, the index "j" can be omitted. It is assumed that the number N_k of harmonic components satisfies the condition:

$$\frac{N_{dt}}{N_k} \geq K_{min}, \quad (21)$$

where the required number of points for determining the harmonic $K_{min} = 16 \div 20$.

The components "A" and "B" compute the amplitudes and phases of the harmonics:

$$F_{\max j(k)} = \sqrt{F_{Aj(k)}^2 + F_{Bj(k)}^2}, \quad (22)$$

$$\phi_{j(k)} = \arctan \frac{F_{Aj(k)}}{F_{Bj(k)}}.$$

The effective values of current and voltage are calculated as *rms* instantaneous values at a constant step:

$$F_{eff.j} = \sqrt{\frac{1}{N_{dt}} \sum_{n=1}^{N_{dt}} F_{j(n)}^2}. \quad (23)$$

The total electrical power consumed or delivered by the motor is found from the effective values of the phase currents and voltages:

$$S_{el} = \sum_{j=1,2,3} I_{eff.j} U_{eff.j}. \quad (24)$$

The active and reactive power consumed or delivered by the PMSM (Permanent magnet synchronous motor) are found from the first harmonic components of the phase currents and voltages [30]:

$$\begin{aligned} P_1 &= \frac{1}{2} \sum_{j=1,2,3} I_{\max j(1)} U_{\max j(1)} \cos(\varphi_{Uj(1)} - \varphi_{Ij(1)}), \\ Q_1 &= \frac{1}{2} \sum_{j=1,2,3} I_{\max j(1)} U_{\max j(1)} \sin(\varphi_{Uj(1)} - \varphi_{Ij(1)}). \end{aligned} \quad (25)$$

The power of asymmetry appears in the case of a phase-by-phase difference in the parameters of the load and is found from:

$$Q_3 = \frac{1}{\sqrt{2}} U_{eff.1} \sqrt{2 \sum_{j=1,2,3} I_{\max j(1)}^2 - \sum_{\substack{g,q=1,2,3 \\ g \neq q}} I_{\max g(1)} I_{\max q(1)} \cos(\varphi_{g(1)} - \varphi_{q(1)})}, \quad (26)$$

where from the sum of the squares of the amplitudes of the first harmonics of the phase currents, all possible combinations of products of these amplitudes are subtracted by the cosines of the differences in the angles of the lagging angles of the first harmonics of the currents from the voltages.

The distortion power consumed or delivered by the motor is found as a quadratic remainder of the total power:

$$Q_2 = \sqrt{S_{el}^2 - P_1^2 - Q_1^2 - Q_3^2}. \quad (27)$$

With the known values of the total power, its components, equivalent to the active resistance of the load, power, shear, distortion and useful factors are calculated.

Formulae for determining the power, shear, distortion, asymmetry and useful factors are:

$$\begin{aligned} k_M &= \frac{P_1}{S_{el}}, \quad k_C = \sqrt{\frac{P_1^2}{P_1^2 + Q_1^2}}, \quad k_2 = \frac{\sqrt{P_1^2 + Q_1^2}}{\sqrt{P_1^2 + Q_1^2 + Q_2^2}}, \\ k_3 &= \frac{\sqrt{P_1^2 + Q_1^2 + Q_2^2}}{S_{el}}, \quad \eta = \frac{3r_l I_{eff.1}^2 + h_{emh} \omega_{rp}}{h_{emw} \omega_{rw}}. \end{aligned} \quad (28)$$

The calculation of aggregate loads in real operational modes is necessary to ensure the reliability of the simulation results and is carried out with the use of the approximation of the available technical characteristics of the units. In particular, for the diesel-generator channel, it is possible to use adjusting characteristics that establish the realizable relationship between the moment on the shaft and its speed [27]. For the tidal power plant assembly, the flow-pressure characteristics of the $Q-H$ are approximated. For example, in the direct-pump mode at the Vislogub tidal power plant 400 kW [31, Fig. 6.1], the characteristic family of the water inflow from the sea into the pool is represented by the formula:

$$Q_P = \sum_{k=1}^4 q_{Pk} H^{k-1}, \quad (29)$$

where, for power, the values of the coefficients $q_p = [- 50 \ 35 \ -2 \ -5] \text{ m}^3/\text{s}$ at a power of 400 kW, and for smaller powers of $q_p(1)$, the value changes from -50 to -32 (Fig. 4). On the basis of the approximation dependences of the type (29), it is possible to determine programmatically the loads of force elements.

Previously mentioned the system operation mode with power from the wind channel, when the available excess capacity of 100 kW is used for pumping water into the pool. If the water level in it is 0.5 m above the sea level, then according to the characteristics (Fig. 4), the productivity will be 15 m^3/s . For the mechanisms under consideration, the cubic dependence of the power and the quadratic moment on the rotational frequency are typical. Therefore, using the known nominal frequency values ω_{0nomp} , and the power P_{pnom} , the required synchronous rotational speed ω_{0p} determining the parameters AI_p , and the corresponding torque h_p on the pump shaft for the mode with power P_p :

$$\begin{aligned} \omega_{0p} &= \omega_{0nomp} \sqrt[3]{\frac{P_p}{P_{pnom}}} = \omega_{0nomp} \sqrt[3]{\frac{100}{400}} = 0,63\omega_{0nomp} = 0,63, \\ h_p &= \frac{P_p}{P_{pnom}} \frac{\omega_{0p}}{\omega_{0nomp}} = 0,25 \cdot 0,63 = 0,4, \end{aligned} \quad (30)$$

where the representation of parameters and physical variables in relative units is used. As a basic mode, the nominal load mode has been taken, according to the parameters of which the basic basis values are adopted (Table 2).

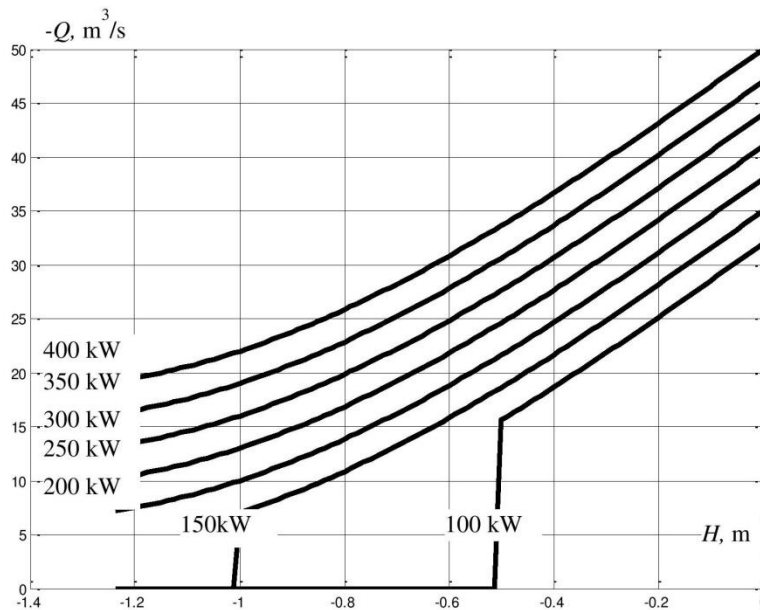


Figure 4. Approximated discharge-pressure characteristics of the tidal aggregate Vislogubskaya TPS (Tidal power station) in the direct pump mode.

In this example, an equivalent three-phase load of 100 kW is realized with the parameters:

$$\begin{aligned} \cos \varphi_l &= 0,707 ; z_l = \frac{3U_{noml}^2 \cos \varphi_l}{P_l R_B} = \frac{3 \cdot 0,707 \cdot 220^2}{100 \cdot 10^3 \cdot 0,257} = 4 ; \\ r_l &= z_l \cos \varphi_l = 2,83 ; l_l = z_l \sin \varphi_l = 2,83. \end{aligned} \quad (31)$$

The filter used in the load circuit is approximately tuned to cancel out 5-7 harmonics and has the parameters in relative units $l_{fl} = 0,286$, $c_{fl} = 3,88$. Reproduction of the static mode with the given data

has given a combination of indicators (Table 3). They show the effective implementation possibility of this and other operation modes of the autonomous power plant complex. Figure 5 shows the calculated phase and load stress diagrams in the static mode under consideration. In the PWM algorithm, a clock frequency of 18 kHz and a modulation frequency of 1,8 kHz have been applied.

Table 2. The parameters of the basic regime and the basic values of the design scheme of the power plant.

Value	Designation	Formula	Value	Unit. am.
Active power of three-phase load	P_l		400	kW
Load power factor	$\cos\varphi_l$		0,707	
Total power of three-phase load	S_l	$P_l / \cos\varphi_l$	566	kVA
Angular Frequency of voltage	f_1		50	Hz
The effective value of phase voltage	U_l		220	V
The effective value of the phase current	I_l	$S_l / (3 U_l)$	857	A
Basic voltage	U_B	$\sqrt{2} \cdot U_l$	311	V
Basic current	I_B	$\sqrt{2} \cdot I_l$	1212	A
Basic angular frequency	ω_B	$2\pi f_1$	314,1593	1/s
The basic angle of rotation	θ_B		1	

Table 3. Integral characteristics of the load channel after the filter in relative units.

$I_{effload}$	$U_{effload}$	$\cos\varphi_{load}$	$S_{ellload}$	$S_{el1load}$	$P_{ellload}$	Q_{1load}	Q_{2load}	k_{mload}	k_{sload}	k_{2load}
0,22	0,7148	0,709	0,4717	0,408	0,289	0,288	0,236	0,614	0,709	0,8655

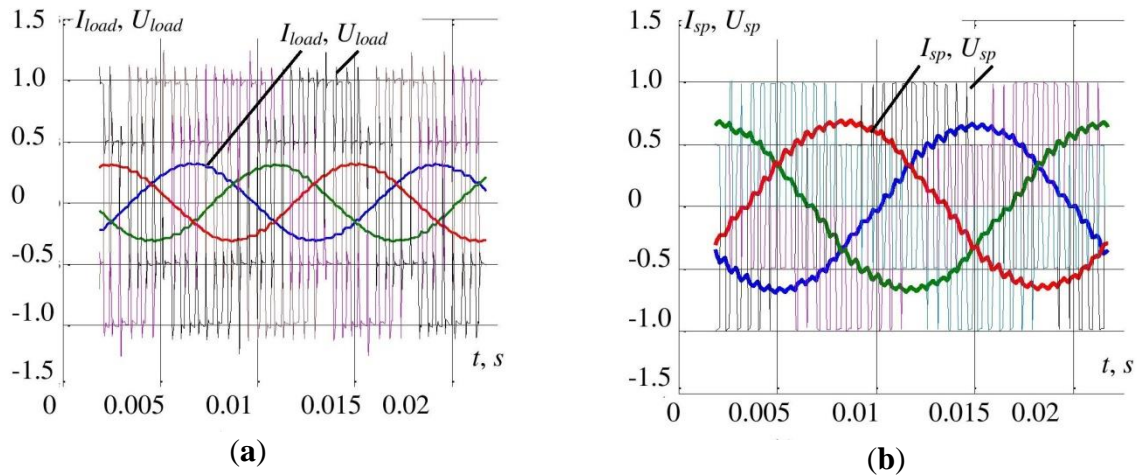


Figure 5. Calculation diagrams of the currents and voltages of the load phases before the filter (a) and stator of the tidal machine in the operating mode of the pump motor (b).

Figure 6 shows the spectra of current harmonics and load voltages in the mode under consideration.

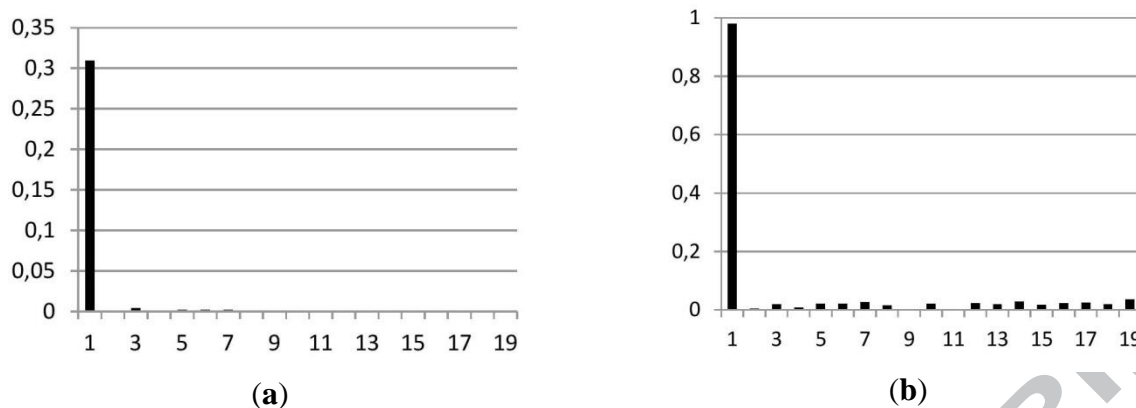


Figure 6. The calculated spectra of the phase current harmonics (a) and the load voltage (b) in the static mode in relative units.

5. Conclusions

A mathematical model of a complex of an autonomous power plant built on the basis of a tidal aggregate and using other sources as a backup has been worked out. Efficient algorithms for mapping the functioning of electric machine aggregates complete with power electronic converters of electric energy parameters have been applied.

The detailed analysis possibility of various operating modes of the units, including the functioning of the tidal aggregate by the turbine and the pump, is illustrated.

The analysis of static and dynamic modes of operation of a power plant and its separate structures on the basis of computer modeling of deterministic and random processes of functioning makes it possible to obtain the necessary information for the selection of technical solutions for the development of energy efficient local power supply systems.

Funding: This research was funded by the state task programme in the sphere of scientific activity of the Ministry of Science and High Education of the Russian Federation (project No. 5.4568.2017/6.7 and No. 13.2078.2017/4.6) and grant of the President of the Russian Federation for state support of the leading scientific schools of the Russian Federation (NSh-2685.2018.5).

Conflicts of Interest: The authors declare that they have no conflict of interest.

References

1. Twidell, J.; Weir, T. *Renewable Energy Resources*. 3rd ed.; Routledge: London and New York, 2015, 784. ISBN 9780415584371.
2. Ivannikova, E.M.; Sister, V.G.; Vasilenko, A.P.; Koltsova, E.S.; Ivannikova, Y.M. Renewables in the Russian Federation and support of the state. *Alternative Energy and Ecology* 2015, 17-18, 172-175, DOI. 10.15518/isjaee.2015.17-18.028.
3. Ellabban, O.; Abu-Rub, H.; Blaabjerg, F. Renewable energy resources: Current status, future prospects and their enabling technology. *Renewable and Sustainable Energy Reviews* 2014, 39, 748-764, DOI: 10.1016/j.rser.2014.07.113.
4. REN21. *Renewables 2017 Global Status Report in perspective*. Renewable Energy Policy Network for the 21st century, 2017, 43.
5. Ocean Energy Forum. *Draft Ocean Energy Strategic Roadmap Building Ocean Energy For Europe*; Technical Report; European Commission: Brussels, Belgium, 2015.
6. Contestabile, P.; Ferrante, V.; Vicinanza, D. Wave Energy Resource along the Coast of Santa Catarina (Brazil). *Energies* 2015, 8, 14219-14243, DOI. 10.3390/en81212423.
7. Falnes, J. A review of wave-energy extraction. *Marine Structures* 2007, 20, 185-201, DOI. 10.1016/j.marstruc.2007.09.001.

8. Tidal Energy. Technology Brief. IRENA Ocean Energy Technology Brief, 3 June 2014, 34.
9. Moghadasi, A.; Sarwat, A.; Guerrero, J.M. A comprehensive review of low-voltage-ride-through methods for fixed-speed wind power generators. *Renewable and Sustainable Energy Reviews* 2016, *55*, 823–839, DOI. 10.1016/j.rser.2015.11.020.
10. Gorji-Bandpy, M.; Azimi, M.; Jouya M. Tidal Energy and Main Resources in the Persian Gulf. *Distributed Generation and Alternative Energy Journal* 2013, *82*, 61-77, DOI. 10.1080/21563306.2013.10677551.
11. Kocaman, A.S.; Abad, C.; Troy, T.J.; Huh, W.T.; Modi, V. A stochastic model for a macroscale hybrid renewable energy system. *Renewable and Sustainable Energy Reviews* 2016, *54*, 688–703, DOI. 10.1016/j.rser.2015.10.004.
12. Li, Y.; McCalley, J.D. Design of a high capacity inter-regional transmission overlay for the US. *IEEE Transactions on Power Systems* 2015, *30*, 513-521, DOI. 10.1109/TPWRS.2014.2327093.
13. Maheshwari, Z.; Ramakumar, R. Smart Integrated Renewable Energy Systems (SIREs): A Novel Approach for Sustainable Development. *Energies* 2017, *10*, 1145, DOI. 10.3390/en10081145.
14. Wan, Y.; Fan, Ch.; Dai, Y.; Li, L.; Sun, W.; Zhou, P.; Qu, X. Assessment of the Joint Development Potential of Wave and Wind Energy in the South China Sea. *Energies* 2018, *11*, 398, DOI. 10.3390/en11020398.
15. Powell, K.M.; Rashid, Kh.; Ellingwood, K.; Tuttle, J.; Iverson, B.D. Hybrid concentrated solar thermal power systems: A review. *Renewable and Sustainable Energy Reviews* 2017, *80*, 215-237, DOI. 10.1016/j.rser.2017.05.067.
16. Renzi, E.; Dias, F. Hydrodynamics of the oscillating wave surge converter in the open ocean. *European Journal of Mechanics-B/Fluids* 2013, *42*, 2-10, DOI. 10.1016/j.euromechflu.2013.01.007.
17. Devolder, B.; Stratigaki, V.; Troch, P.; Rauwoens, P. CFD Simulations of Floating Point Absorber Wave Energy Converter Arrays Subjected to Regular Waves. *Energies* 2018, *11*, 641, DOI. 10.3390/en11030641.
18. Mustafa, Sh.S.; Misron, N.; Lutfi, O.M.; Tsuyoshi, H. Power Characteristics Analysis of a Novel Double-Stator Magnetic Geared Permanent Magnet Generator. *Energies* 2017, *10*, 2048, DOI. 10.3390/en10122048.
19. Zhang, L.; Li, M. Bond graph modeling and fault diagnosis of tidal turbine systems. *Conference Chinese Control* 2016, Chengdu, China, 6826 – 6831, DOI. 10.1109/ChiCC.2016.7554431.
20. Ghefiri, K.; Bouallègue, S.; Haggège, J.; Garrido, I.; Garrido, A. Firefly algorithm based-pitch angle control of a tidal stream generator for power limitation mode. *IC ASET* 2018, Hammamet, Tunisia, 387 – 392, DOI. 10.1109/ASET.2018.8379887.
21. Li, X.; Wang, H.; Zhao, H.; Bao, H. Numerical simulation of the viscous flow around duct of tidal turbine. *International Conference on Electrical and Control Engineering* 2011, Yichang, China, 1637 – 1640, DOI. 10.1109/ICECENG.2011.6058396.
22. Vujacic, M.; Hammami, M.; Srdovic, M.; Grandi, G. Theoretical and Experimental Investigation of Switching Ripple in the DC-Link Voltage of Single-Phase H-Bridge PWM Inverters. *Energies* 2017, *10*, 1189, DOI. 10.3390/en10081189.
23. Bierhoff, M.H.; Fuchs, F.W. DC-link harmonics of three-phase voltage source converters influenced by the pulsewidth-modulation strategy –An analysis. *IEEE Transactions on Industrial Electronics* 2008, *55*, 2085–2092, DOI. 10.1109/TIE.2008.921203.
24. Aboul-Seoud, T.; Sharaf, A. A novel Dynamic Voltage Regulator compensation for a stand alone tidal energy conversion scheme. *IEEE Electrical Power & Energy Conference* 2010, Halifax, NS, Canada, 1 – 6, DOI. 10.1109/EPEC.2010.5697210.
25. Aboul-Seoud, T.; Sharaf, A. Utilization of the Modulated Power Filter Compensator scheme for a grid connected rural hybrid wind/tidal energy conversion scheme. *IEEE Electrical Power & Energy Conference* 2010, Halifax, NS, Canada, 1 – 6, DOI. 10.1109/EPEC.2010.5697211.
26. Tekobon, J.; Chabour, F.; Nichita, C. Development of HILS emulator for a Hybrid Wind — Tidal Power System. *CISTEM* 2016, Marrakech, Morocco, 1 – 8, DOI. 10.1109/CISTEM.2016.8066821.

27. Baykov, A.I.; Dar'enkov, A.B.; Sosnina, E.N. Simulation modeling of wind-diesel power station. *Russian Electrical Engineering* 2018, 3, 26-33. DOI. 10.3103/S1068371218030033
28. Khan, S.S.; Tedeschi, E. Modeling of MMC for Fast and Accurate Simulation of Electromagnetic Transients: A Review. *Energies* 2017, 10, 1161. DOI. 10.3390/en10081161.
29. Gorev, A.A. *Transient processes of a synchronous machine*; State Energy Publishing House: Leningrad-Moscow, Russia, 1950; 552.
30. Maevskiy, O.A. *Power characteristics of gate converters*; Energiya: Moscow, Russia, 1978; 320.
31. Bernshtein, L.B.; Silakov, V.N.; Gelfer; S.L. *Tidal power plants*; Energoatomizdat; Moscow, Russia, 1987; 296.